Sustainable Chemical Engineering
https://ojs.wiserpub.com/index.php/SCE/

UNIVERSAL WISER PUBLISHER

Research Article

Morphological, Thermal, Physicomechanical and Optical Properties of Crosslinked Poly (Ester-Urethane-Acrylate): Effect of Added Methyl Methacrylate

Shyam Dev Maurya[1*], Sanjay K. Nayak[2]

[1]Department of Research and Development, Super Bond Adhesive Pvt. Ltd, Mumbai, India
[2]Department of Chemistry, Ravenshaw University, Cuttack, Odisha, India
Email: shyam4ucipet@gmail.com

Received: 29 February 2024; **Revised:** 2 April 2024; **Accepted:** 3 April 2024

Abstract: Poly (ester-urethane-acrylate) (PEUA) macromonomer was prepared by reacting two moles of isophorone diisocyanate (IPDI) with one mole of bis (1,4-butanediol ortho-phthalate) (BPE), followed by end-capping with two moles of 2-hydroxyethyl methacrylate (HEMA) in the presence of a dibutyltin dilaurate (DBTDL) catalyst. Thereafter, different ratios of methyl methacrylate (MMA) were added to the PEUA macromonomer to prepare crosslinked PEUA/MMA sheets. Fourier transform infrared spectrometry (FTIR), ultraviolet-visible spectrophotometry (UV-vis), and differential scanning calorimetry (DSC) techniques were employed to investigate the structure, optical transparency, and thermal properties of the crosslinked sheets. The effect of MMA on the polymerization shrinkage and abrasive wear properties of PEUA and their copolymers was also studied. The polymerization shrinkage study showed that the PEUA copolymer containing 40 wt% MMA had a more rigid microstructure with improved volume shrinkage and abrasive wear properties as compared with the other compositions of PEUA copolymers with MMA loadings of 80, 60, and 20%. The improvement was attributed to the better miscibility and compatibility of 40 wt% MMA with PEUA, as revealed by DSC, heat deflection temperature (HDT), and scanning electron microscope (SEM) studies.

Keywords: poly (ester-urethane-acrylate), polymerization shrinkage, abrasive wear rate, optical properties, glass transition temperature

1. Introduction

Polyurethane-acrylate (PUA) macromonomers find applications in various areas including printing ink, coatings, stereo-lithograph (3D Printing), adhesives, paints, transparent sheets and dental materials.[1-5] The PUA prepolymer can be synthesized by the reaction of an isocyanate with a compound containing hydroxyl groups, like a polyol, followed by end capping with acrylate.[6] The isocyanate forms the hard segments of PUA that are responsible for its rigidity, whereas the soft segments, composed of polyether or polyester polyols, account for the flexibility of the backbone. The nature and structure of PUA and its physical as well as mechanical properties depend on the nature of the backbone and end groups of the acrylate. Various preparation methods, such as copolymerization, interpenetrating polymer networks (IPN), blending, etc., have been reported to improve the physical, optical, mechanical and thermal properties of polyurethane acrylate films.[7-10]

DOI: https://doi.org/10.37256/sce.5220244532

Amongst the above methods, copolymerization is the most promising approach for altering the properties of polymeric materials for different applications. Despite many advantages of PUA copolymerization, the greatest limitation is its molding process resulting in volume shrinkage during curing. The shrinkage, for instance, results in the formation of residual stress on a PUA adhesive-adhered interface which, in turn, leads to the formation of microvoids and interfacial gaps. The polymerization shrinkage can be controlled to an extent by varying the composition of the monomers. Many authors have studied the effect of added comonomers, such as MMA and styrene, on the volume shrinkage of the PUA. For instance, Lin et al.[11] showed that the styrene affected the volume shrinkage of 2-hydroxyethyl-methacrylate-polyurethane (polypropylene glycol)/styrene (HEMA-PU(PPG)/styrene) system which was closely correlated to the microstructure of the crosslinked structure. Apart from the volume shrinkage, the abrasive wear behavior is another important property of polyurethanes, as it is concerned with an end-use property. Abrasive wear results in the loss of material by the dynamic interaction between the two surfaces, resulting in the removal of material from the polymer surface. The abrasive wear properties of polymeric materials can be improved by the formation of a rigid network structure.[12] The mechanical properties of urethane-acrylate can be improved by the incorporation of various reactive diluents, or comonomers, such as ethyl acrylate, MMA, acrylonitrile, etc. through copolymerization.[11,13] Among these diluents, MMA monomer has been extensively used for the copolymerization of PUA due to its good compatibility and low toxicity and resulting in excellent transparency and sheet fabric formation ability. The PEUA/MMA gives better abrasion resistance properties due to the crosslinked network structure formed by strong hydrogen bonding.[2]

Thus, the primary aim of the current research was to synthesize PEUA/MMA copolymers by incorporating different concentrations of MMA. Thereafter, the PEUA/MMA copolymers were subjected to various characterization techniques, such as FTIR, UV-vis, DSC and SEM, to evaluate the volume shrinkage and abrasive wear properties along with the mechanical, thermal, optical and morphological properties of the PEUA/MMA.

2. Experimental

2.1 *Materials*

Methylmethacrylate (MMA) was procured from Himedia Laboratories Ltd. (India). Phthalic anhydride (PA), 2-hydroxyethyl methacrylate (HEMA), tetrabutyl orthotitanate ($Ti(OBu)_4$), dibutyltin dilaurate (DBTDL) and isophorone diisocyanate (IPDI) were purchased from Sigma Aldrich Co. (United State of America). 1,4 butanediol (BDO) was purchased from Augustine Chemicals Inc. (United States of America). Azobisisobutyronitrile (AIBN) was obtained from Sisco Research Laboratories Pvt. Ltd. (India) and was recrystallized twice using chloroform. All other common solvents used were analytical grade.

2.2 *Synthesis of crosslinked poly (ester-urethane-acrylate) and copolymers*

Aromatic bis (1,4-butanediol ortho-phthalate) (BPE), used as a hydroxyl-terminated ester, was synthesized as described in previous literature papers by reacting 1 mol of phthalic anhydride (PA) with 2 moles of 1,4-butanediol (BDO) using Ti $(OBu)_4$ as a catalyst.[3,14] PEUA macromonomer was then synthesized as depicted in Figure 1. A mixture of 10.87 g BPE (0.035 mol), along with 0.22 g DBTDL catalyst (0.35 mmol) was placed in a 500 ml three-necked round-bottom flask fitted with a magnetic stirrer and a nitrogen inlet valve. After that 15.56 g IPDI (0.07 mol) was added to the BPE, dropwise by a syringe pump, to obtain NCO-terminated urethane and then capped by 9.1 g HEMA (0.07 mol) to obtain the PEUA prepolymer. A similar route was used for the preparation of PEUA/MMA copolymers using varying amounts of the MMA. Further, crosslinked sheets of PEUA and PEUA/MMA copolymers were prepared in the presence of AIBN (1% w/w) free radical initiator added to the prepolymers. The prepolymer was poured into a glass mold having dimensions 320 × 230 mm, and the thickness of the sheet was controlled using a 3 mm gasket. Further, the glass mold was kept at 60 °C in an air-oven overnight and the post-cured at 80 °C for 3 hours.[15] The samples were designated as PEUA, PEUA-1, PEUA-2, PEUA-3 and PEUA-4, where the numbers 1, 2, 3 and 4 denote 80, 60, 40 and 20 wt% of MMA, respectively, whereas PEUA contains no MMA.

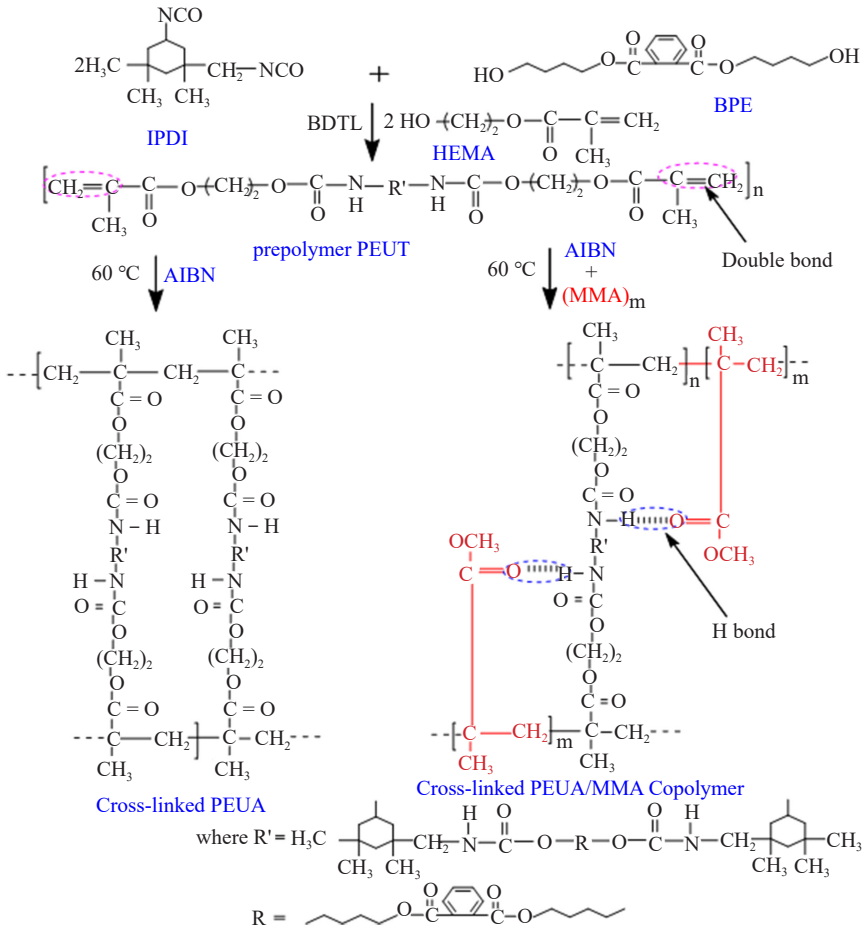

Figure 1. Schematic representation of the synthesis of PEUA and the crosslink structures of PEUA and the PEUA/MMA copolymer

3. Characterization

3.1 *Attenuated total reflectance-Fourier transform infrared spectroscopy (ATR-FTIR)*

The attenuated total reflectance-Fourier transform infrared spectroscopy (ATR-FTIR) spectra of PEUA and its copolymers were recorded on a Nicolet 6,700, Thermo Fisher Scientific Co. United States of America, with Ominic software for data collection in the standard wave range of 4,000-400 cm^{-1}. All the spectra were obtained at 4 cm^{-1} resolution and 64 consecutive scans.

3.2 *UV-visible spectroscopy*

UV-visible spectra of PEUA and its copolymer samples were recorded and the optical transparency was determined using a double beam spectrometer 2,450 PC Series, Shimadzu Corp. (Japan), with an integrating sphere assembly. FTIR focuses on vibrational transitions in the infrared region, while UV-visible spectroscopy probes electronic transitions in the ultraviolet region.

3.3 *Crosslinke density*

The crosslink densities of the samples were determined by measuring the ratio of the weight of the sample to the displaced volume of the water employing the following equation 1. The samples of dimensions (10 × 30 × 2.8 mm^3), prepared by a hacksaw cutting machine, were used for the analysis and the average values of five samples were recorded.

$$\rho = \frac{m}{m - m_1} \times \rho_0 \quad (1)$$

Where ρ_0 is the density of the liquid, m is the weight of the samples measured in air and m_1 is the weight of the sample immersed in the liquid.

3.4 *Polymerization shrinkage*

The volume shrinkage of the free radical polymerized samples was investigated by using equation 2:[16]

$$Polymerization\ Shrinkage(\delta)(\%) = \frac{(\rho_{polymer} - \rho_{monomer})}{\rho_{polymer}} \times 100 \quad (2)$$

where ρ is the density of the specified sample.

The theoretical polymerization shrinkage (δt) of a copolymer is calculated by the volume additive principle which states that ($\delta t\% = w_1\delta_1 + w_2\delta_2$) where $\delta t\%$ is the shrinkage percent of the copolymer, w_1 and w_2 are the weight fractions of the constituents, prepolymer and MMA, respectively, and δ_1 and δ_2 are the shrinkage values for the pure PMMA and PEUA.[17] The densities of the monomers ($\rho_{monomer}$) were measured by using a graduated cylinder at 25 °C. The density of the cross-linked sheet was determined by the displacement method, using a Mettler Toledo (Switzerland) weighing balance and a density measurement kit, ME-DNY-43. The polymerization shrinkage ($\Delta\delta$) was calculated by the differences of experimental (δe) and theoretical (δt).

3.5 *Double bond concentration*

The concentration of double bonds (C_{db}) summed overall mers in the PEUA/MMA segments was calculated by using equation 3:

$$Concentration\ of\ double\ bonds\ (C_{db}) = \frac{Functionalities\ of\ the\ mers \times mers\ density}{molecular\ weight\ of\ mers} \quad (3)$$

The functionalities of the mers were one for MMA and two for PEUA.

3.6 *Void contents*

The void fractions of the sample were calculated using equation 4:

$$Void\ contents = \frac{\rho_{theo} - \rho_{exp}}{\rho_{theo}} \quad (4)$$

where $\rho_{theo.}$ = theoretical density of the copolymer and $\rho_{exp.}$ = experimental density of the copolymer.

The difference in the values of experimental and theoretical density is a measure of the presence of voids in the copolymer. The theoretical density of the copolymer was calculated by the volume additive principle method based on the densities of pure PMMA and PEUA (Table 2).[17]

3.7 *Abrasive wear analysis*

The abrasive wear characteristics of PMMA, PEUA and its copolymers were studied using an abrasion tester machine, model 5131, Taber Industries (United States of America). The test was conducted using discs of 100 mm diameter and 2.8 mm thickness prepared *via*. a hacksaw cutter from the crosslinked sheet. The circular specimens were held against the rotating flat platform of the abrasive wear machine at a constant load (4.9 Newtons) by two stationary abrasive wheels one on each side shown in Figure 2, which resulted in a circular ring on the rotating specimen surface with an abrasion area of 30 cm^2. The rasping action between the sample and the abrasive wheels during the rotatory

motion of the machine resulted in the loss of material from the specimen surface. Materials of higher wear resistance will have a lower volume loss. The test was conducted using CS-10 wheels at a constant load of 4.9 Newtons, rotating at a fixed speed of 4.4 m/s. The weight loss was measured using a microbalance with an accuracy level of 0.0001 g. The specific wear rates were calculated from the weight loss of the sample by using equation 5.[18]

$$\Delta W = W_1 - W_2 \tag{5}$$

where ΔW is weight loss of the sample, W_1 is the weight of the sample before the test and W_2 is the weight of the sample after the test.

The volume loss (ΔV) of the sample was calculated using equation 6:

$$\Delta V = \frac{(W_1 - W_2)}{\rho} \times 1000 \tag{6}$$

where ρ is the density of the sample.

The specific wear rates (W_s) of the samples were calculated using equation 7:

$$W_s = \frac{\Delta V}{F_n \times A_d} \tag{7}$$

where A_d = Abrasive distance (m) and F_n = normal load (4.9 N)

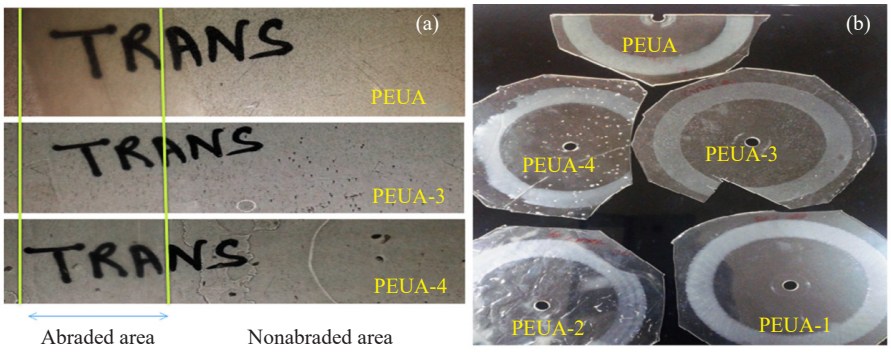

Figure 2. Photographs of (a) transmission of the abrasive surfaces of the PEUA, PEUA-3 and PEUA-4 and (b) the abraded surfaces of all samples

3.8 *Scanning electron microscopy (SEM)*

The surface topographies of the worn surface of the PEUA and its copolymers were studied using a scanning electron microscope EVO 15, CARL ZEISS (Germany). Prior to imaging the samples were sputter coated with platinum.

3.9 *Chemical resistance analysis*

The chemical resistance of PEUA and its copolymers were determined according to a previously described procedure.[2,10] The crosslinked PEUA and its copolymer samples were immersed in various chemical reagents (viz. 10% NaOH, 10% HCl, 10% H_2SO_4, 10% CH_3COOH, 10% HNO_3, toluene and xylene) at 25 °C for seven days. Subsequently, the samples were taken out of the solvent bath, wiped with tissue paper to remove the adhered solvent, and weighed immediately. The percentage change was calculated using equation 8:

$$Percent\ change\ (\%) = \frac{W - W_1}{W_1} \times 100 \tag{8}$$

where W_1 is the initial weight (g) of the sample and W is the final weight (g) of the sample after seven days.

3.10 *Heat deflection temperature (HDT) ananlysis*

The heat deflection temperature (HDT) tests of PEUA, PMMA and the copolymers were conducted using an HDT analyzer HV-2000A-C3 (Gotech Testing Machine, Taiwan) as per ASTM D 648. The test was carried out in flexural mode using rectangular specimens cut from the crosslinked sheets (via a counter cutter machine) of dimension 127 mm × 12.7 mm × 2.8 mm with a load of 0.455 MPa and at a heating rate of 2 °C/min.

3.11 *Differential scanning calorimetry (DSC) analysis*

The thermal properties of PEUA and PEUA-3 were determined using a DSC Q 20 Differential scanning calorimeter (TA Instrument co. U.S.A.). Samples of ≤ 8 mg were heated from -70 to 200 °C at a heating rate of 10 °C min^{-1} in a nitrogen atmosphere.

There are many models presented in the literature for compatability and miscibility, based on the glass transition temperatures of a copolymer.[19] The composition dependence of T_g was obtained from the DSC analysis. The glass transition temperature of a copolymer is calculated from the T_g of the individual polymers by the Fox equation 9:[20]

$$\frac{1}{T_g} = \frac{W_1}{T_g^1} + \frac{1-W_1}{T_g^2} \tag{9}$$

where T_g is the glass transition temperature of the copolymer. T_g^1 is the glass transition temperature of PEUA, T_g^2 for PMMA, W_1 is the weight fraction of PEUA and $1-W_1\left(=W_2\right)$ is the weight fraction of PMMA. Equation (9) is symmetric with respect to the two components of the polymer and allows the prediction of virgin polymer (PEUA and PMMA) properties.

A related equation is the Gordon and Taylor (GT) equation 10:[21]

$$T_g = \frac{W_1 T_g^1 + k\left(1-W_1\right)T_g^2}{W_1 + k\left(1-W_1\right)} \tag{10}$$

where k is evaluated from the experimental data.

4. Results and discussion

4.1 *FT-IR analysis*

Figure 3 displays the FTIR spectra of IPDI, BPE, the HEMA-IPDI-BPE-IPDI-HEMA (PEUA = prepolymer), PEUA-3 (prepolymer before crosslinking) and crosslinked PEUA-3 copolymer. The major characteristic absorbtion peaks are assigned in Table 1.

An absorption band at 2,251 cm^{-1} is assigned to the NCO groups of the diisocyanate (Figure 3, curve a). A broad peak for the -OH groups at 3,300 cm^{-1}, C=O groups at 1,716 cm^{-1}, aromatic rings at 1,599 cm^{-1}, ortho disubstituted benzene groups[22] at 740 cm^{-1} and CH_2 stretch at 2,700-3,000 cm^{-1} confirmed the formation of BPE (Figure 3, curve b). Figure 3, curve c shows the appearance of C=O stretching at 1,712 cm^{-1} along with the -NCO stretching at 2,251 cm^{-1} showing the initial reaction of IPDI and BPE in the PEUA prepolymer. The disappearance of the NCO peak and appearance of C=C stretch at 1,637 cm^{-1} and the methyl group of the HEMA at 1,451 cm^{-1} confirmed the completion of the reaction and the formation of the PEUA prepolymer, as shown in Figure 3, curve d. The absorption peaks at 1,385 cm^{-1} and 1,451 cm^{-1} confirmed the presence of methyl groups of either MMA and HEMA to be present in the copolymer (Figure 3, curve e).[10] Finally, the disappearance of C=C stretch at 1,637 cm^{-1} and 815 cm^{-1} and the appearance of C-O-C stretching peak at 1,236 cm^{-1} and 1,099 cm^{-1} confirmed the formation of the crosslinked PEUA structure in Figure 3, curve f.

Table 1. Assignment of the characteristic IR peaks

Absorption Bands (cm^{-1})	Assignment
3,373	N-H hydrogen-bonded to urethane > C=O
3,300	Stretching of O-H in polyols
2,960-2,800	CH_2 stretching (asymmetric and symmetric)
2,251	Stretching of N=C=O
1,720	Free C=O
1,708	Urethane C=O hydrogen bonded to N-H
1,637	Stretching of C=C
1,599	Vibration of aromatic ring
1,530	Stretching of N-H of urethane
1,460	Bending of CH_2
1,451	CH_3 stretching of HEMA
1,385	CH_3 stretching of MMA
1,125	Stretching of C-O-C
816	Stretching of C=C
773	Aromatic C-H
740	Vibration of ortho position aromatic

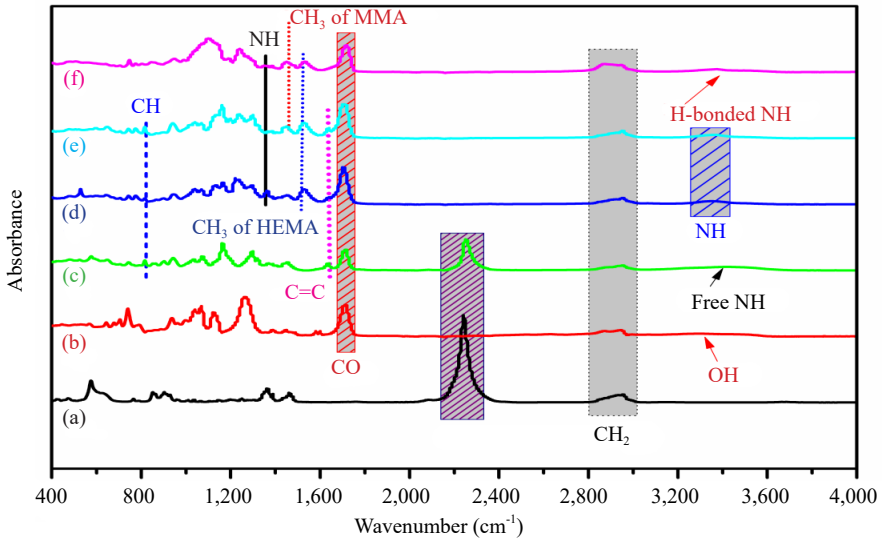

Figure 3. FTIR spectra of: (a) isophorane diisocyanate (IPDI) (b) bis (1,4-butanediol ortho-phthalate) (BPE) (c) Initial IR of PEUA prepolymer (d) PEUA prepolymer (e) PEUA-3 prepolymer (f) PEUA-3 crosslinked sheet

Figure 4 shows the results of FTIR studies of all the crosslinked copolymers carried out by focusing on the three main regions, -CH stretching at 2,960-2,800 cm^{-1}, C=O stretching at 1,730-1,690 cm^{-1} and the -NH stretching at 3,500-3,300 cm^{-1}.[2] Polyurethanes are capable of forming several kinds of hydrogen bonds due to the presence of a C=O acceptor group and a -NH donor group in the urethane linkages. The related stretching bands have been extensively used to describe the presence of H-bonds and correlate with the miscibility and compatibility of the copolymer.

Figure 4a presents the FTIR spectra of the crosslinked samples for analyzing the strength of the H-bonds. Virgin PEUA had two intense -C=O peaks and a broader urethane -NH peak. The broader -NH stretching vibrations band is

due to hydrogen bonded -NH (3,355 cm^{-1}), while the C=O bonds correspond to hydrogen bonded at (1,690-1,730 cm^{-1}) in Figure 4b.[23]

The specific peak positions of -NH groups and -C=O groups for the various copolymers are shown in Figure 4c and b. For PEUA-1 and PEUA-2 the appearance of the N-H bands between 3,600-3,300 cm^{-1} (Figure 4c) indicated the bonded and nonbonded hydrogen groups respectively. In the case of PEUA-3, the appearance of the -NH peak at 3,352 cm^{-1} suggested that most of its -NH groups were hydrogen bonded whereas PEUA-4 showed only a very low intenity NH peak due to an incomplete and non-uniform network structure (Figure 4a and c). The -C=O band stretching mode appeared at 1,695 cm^{-1} (Figure 4b) for PEUA and at 1,719-1,701 cm^{-1} for the PEUA copolymer, due to the greater electron delocalization of the π-bonds there in the former. In addition, PEUA-1 had a relatively sharp -C=O peak due to the large dipoles of its carbonyl bonds. Thus, the concentration of MMA in PEUA played an important role in determining the strength of hydrogen bonding in the copolymer. The increase in peak intensity and peak position of the -NH and -CO groups clearly indicates the formation of a complete and uniform network structure for the PEUA-1, PEUA-2 and PEUA-3.

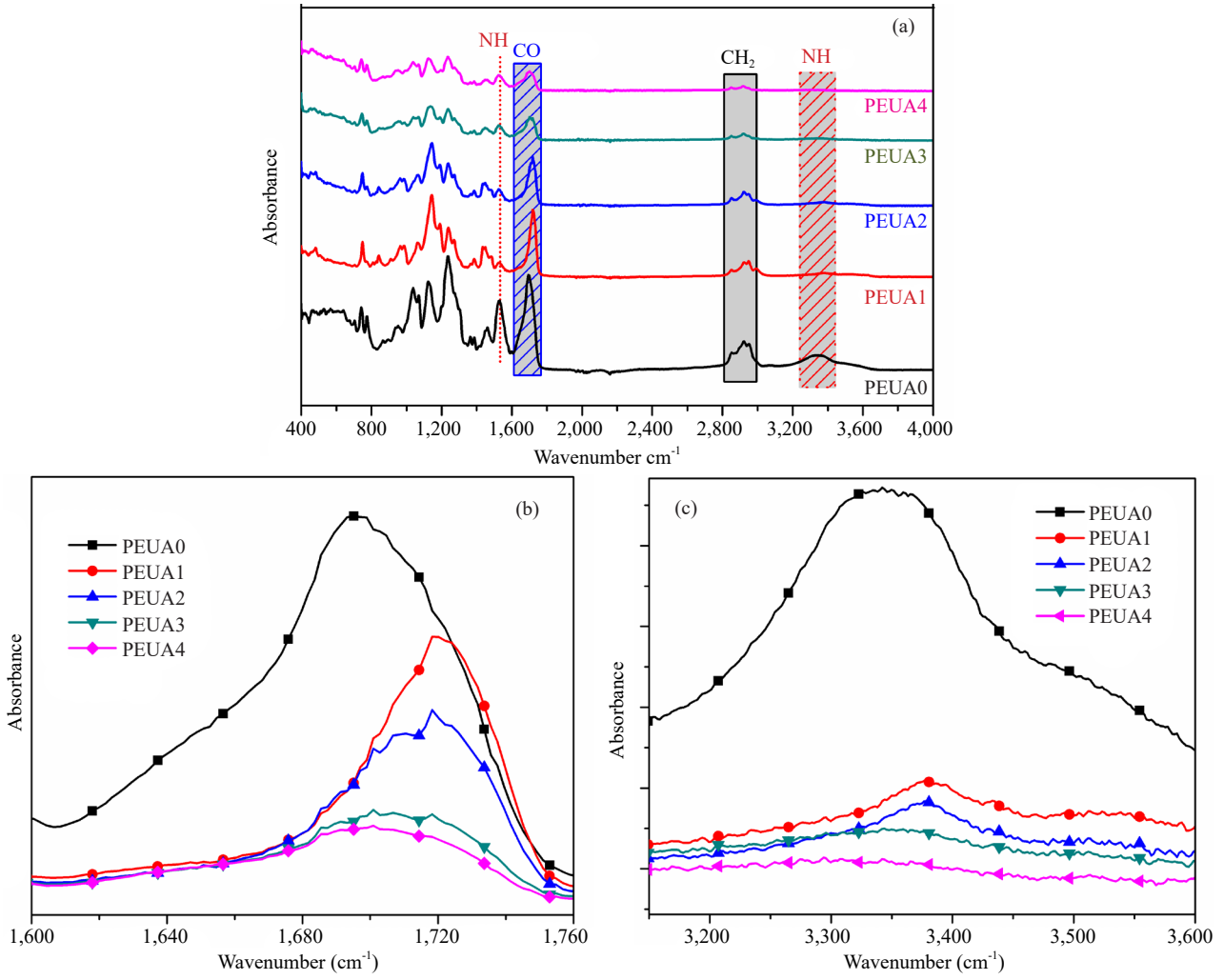

Figure 4. The FTIR spectra of (a) the crosslinked PEUA/MMA copolymers (b) CO absorbance regions for the copolymers and (c) NH absorbance regions for the copolymers

4.2 *Polymerization shrinkage*

Volume shrinkage occurs during polymerization and crosslinking of copolymers due to the conversion of large

numbers of monomers into a smaller number of polymer molecules. The type of co-monomer used changes the shape and size of the polymer molecule, affecting the volume shrinkage. The volume shrinkage of pure PEUA was found to be 7.3% during its polymerization whereas pure PMMA shrunk by about 21%.[24] The variation in shrinkage of the copolymer with composition is shown in Table 2. It is evident from the data that the PEUA-1, PEUA-2 and PEUA-3 showed positive $\Delta\delta$ values which indicates the formation of a rigid network due to the compatibility of PEUA and MMA. However, the PEUA containing 40 wt% MMA (PEUA-3) showed a more rigid network, as compared to the other copolymers due to its higher crosslink density, confirmed by the micrograph analysis discussed in a later section. In addition, PEUA-4 (20 wt% MMA) showed a negative $\Delta\delta$ value, i.e. -1.68, which is attributed to the formation of a loosely bonded network structure in this copolymer.[11] In addition, to reduced shrinkage, the PEUA copolymer offered improved properties i.e. abrasive wear resistance, chemical resistance and service temperature, as described in the next section.

Table 2. Cross-link density and polymerization shrinkage of PEUA, PMMA and PEUA/MMA copolymers at 60 °C

Sample (PEUA/MMA)	Cross-link density	Polymerization shrinkage (δ) (%)		Difference	Voids
	(g/cc)	Experimental (δ_e)	Theoretical (δ_t)	$\Delta\delta = \delta_e - \delta_t$	
PEUA	1.175	7.29	-	-	-
PMMA	1.189	20.96	-	-	-
PEUA-1 (20:80)	1.194	20.09	18.22	1.87	-0.0063
PEUA-2 (40:60)	1.195	16.01	15.49	0.52	-0.0101
PEUA-3 (60:40)	1.197	12.83	12.75	0.08	-0.0137
PEUA-4 (80:20)	1.176	8.34	10.02	-1.68	0.0017

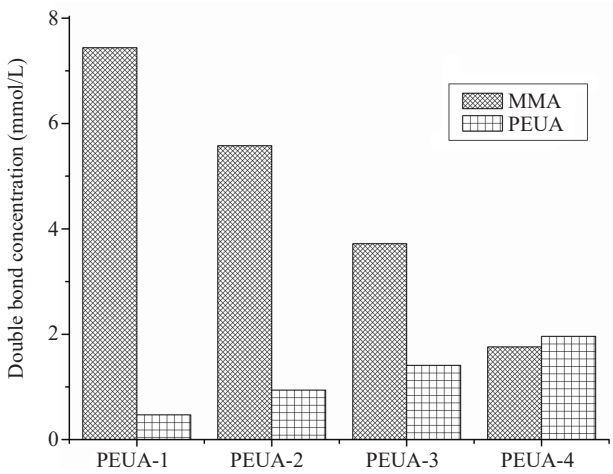

Figure 5. Double bond concentrations in the MMA and PEUA segments for the PEUA/MMA copolymers

Another dominant factor which influences the volume shrinkage is the concentration of double bonds. Using eqn. 3 the double bond concentrations of the MMA mers and PEUA were 0.0093 mmol/liter and 0.0023 mmol/liter, respectively in all the copolymers. The volume shrinkage depends to a major extent on the concentration of double bonds because an increase in double bonds in a copolymer increases the volume shrinkage.[25] It can be observed from Figure 5 that all the PEUA components exhibited lower double bonds because of their structure, and this concentration as compared to the MMA monomer in the copolymers except PEUA-4. For PEUA-4 the concentration of the double bonds in the 80% PEUA segments (1.96 mmol/liter) was higher than in the 20% MMA (1.76 mmol/liter) segments,

indicating that a few double bonds of PEUA did not react in the copolymer. This observation might be due to the lower reactivity of PEUA towards MMA. This results in lower crosslinking density and more voids in PEUA-4 which can be correlated with the findings of Wen et al.[26] Hence, from the above results it was confirmed that the monomer concentration influenced the resulting double bond concentrations due to monomer size and polymerization shrinkage i.e. decreasing the MMA concentration decreased the double bond concentration as well as the polymerization shrinkage.

4.3 *Abrasive wear behavior*

The volume loss and specific abrasive wear rate of PEUA and its copolymers are listed in Table 3. It was observed that the wear rate of the PEUA samples decreased with decreasing MMA content except for PEUA-4. This attribute to the decrease in concentrations of MMA leading to negative polymerization shrinkage. The improvement (decrease) of the specific wear rate indicated that PEUA-3 had the best interaction between PEUA and MMA, attributed to its highest crosslink density shown in Table 2. This was ascribed to the presence of a condensed microstructure of the PEUA-3 copolymers. Another possible reason for the reduced abrasion wear rate in the PEUA copolymer with decreasing MMA up to PEUA-3. Moreover, the presence of more H-bonds in PEUA-3, as observed through the FTIR studies, might also be a plausible reason behind the formation of a rigid network structure and reduced abrasive loss. However, in PEUA-4 all double bonds in PEUA did not react due to the lower concentration of MMA, resulting in the formation of a loose network structure. Figures 4 a and b show comparative photographs of the abrasive wear samples which clearly indicate that PEUA-3 exhibited better transparency as compared to PEUA and PEUA-4.

Table 3. Volume loss and specific wear rate of PEUA and the copolymers (at constant weight: 4.9 N, abrasive width 6.35 mm, abrasive velocity: 0.072 m/sec, abrasive distance: 72 m)

Sample	Volume loss (ΔV) × 10^{-5} (mm^3)	Specific wear rate (mm^3/N.m) × 10^{-6}
PEUA	5.16	0.143
PEUA-1	2.68	0.075
PEUA-2	2.16	0.060
PEUA-3	1.75	0.049
PEUA-4	4.01	0.111

4.4 *Scanning electron microscopy (SEM) analysis of PEUA and its copolymers*

In order to understand the mechanism of the abrasive wear behavior of PEUA and its copolymers, SEM analysis was used to probe the morphology of the worn surface, as shown in Figure 6. Abrasion wear resulted from the microploughing action of the abrasive wheel, resulting in the appearance of all the worn surfaces as shown in Figure 2.

The quantitative determination of wear showed that the wear volume of the copolymer steadily decreased with increasing PEUA content up to PEUA-3, whereas the reverse was observed in PEUA-4. The highest roughness of the surface was found in pristine PEUA, whereas it was the least in PEUA-3. The small scratches-like patterns observed on the abrasive wear surface of PEUA-3 appeared to be shallow and limited to thin layers, which suggests a microcracking mechanism (Figure 6d). PEUA-4 showed more worn surface, pits and clefts due to its loose microstructure (Figure 6e). The most improved abrasive wear resistance, obtained in PEUA-3, was attributed to the good compatibility and miscibility between the PEUA and MMA.[27-30] Thus, the worn surface also correlates with the finding of abrasion wear and loss of transparency results discussed above.

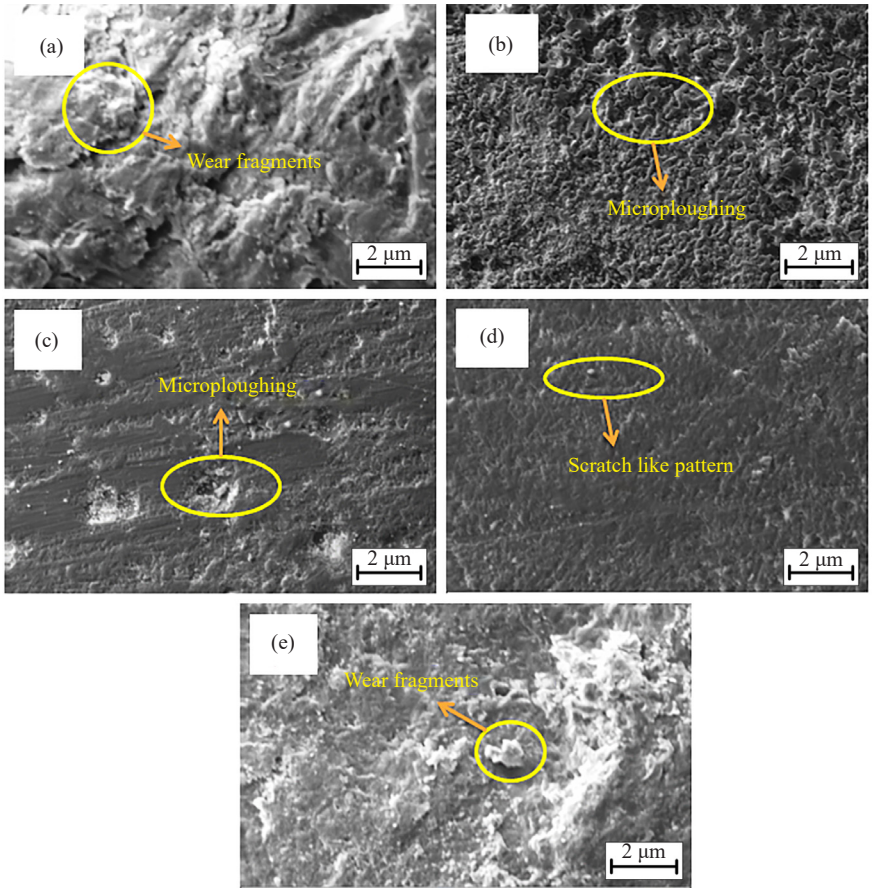

Figure 6. SEM micrograph of the inside of the worn surface of the samples after abrasion for the 72 meter distance (a) PEUA (b) PEUA-1 (c) PEUA-2 (d) PEUA-3 and (e) PEUA-4

4.5 *Chemical resistance properties*

To evaluate the chemical resistance of PEUA and its copolymers, they were subjected to acid and alkali reagents according to a weight gain percent method.[2] From the data tabulated in Table 4 all the copolymer samples gained weight in acids and alkalis and, thus had excellent resistance. The better chemical resistance behavior of the PEUA/MMA copolymers as compared to PEUA could be due to the addition of MMA.[30] The slightly higher wt% changes in PEUA were probably due to the hydrophilic polar groups (urethane and ester groups) in the backbone which underwent solvolysis.[31] However, PEUA-1 showed the maximum percent change in toluene and xylene which was due to the high wt% of MMA due to PMMA being soluble in both then would be wt% loss. PEUA-3 showed very little wt% change in all the chemicals except toluene and xylene, due to its dense structure as discussed earlier that hinders the penetration of the chemicals.

Table 4. Percent change in weight of PEUA and its copolymer after 7 days submersion at room temperature in various chemical reagents

Composition	10% NaOH	10% HCl	10% H_2SO_4	10% CH_3COOH	10% HNO_3	Toluene	Xylene
PEUA	1.91	1.83	2.02	2.71	2.18	0.10	0.03
PEUA-1	0.50	0.43	0.48	0.57	0.55	35.88	30.24
PEUA-2	0.46	0.47	0.42	0.60	0.42	3.43	3.10
PEUA-3	0.37	0.40	0.40	0.43	0.34	0.12	0.05
PEUA-4	0.38	0.52	0.83	0.51	0.42	0.07	0.02

4.6 *UV-visible spectroscopy*

The UV-visible spectra of PEUA and its copolymers are depicted in Figure 7 and the results are summarized in Table 5. It is obvious that all the copolymers had high transmittance, above 97%, in the visible regions at λ ≈ 550-600 nm, but PEUA-1 exhibited the highest value as compared to the other copolymers due to the higher content of PMMA which absorbs only a trace amount of light and UV radiation. On the other hand, PEUA-4 showed the lowest transparency at λ ≈ 450-550 nm as compared to the other copolymers, which may be due to loose structure. The above findings can be correlated with the work reported by several authors.[32-34] Taiichi et al.[32] for instance, showed increased transparency in urethane dimethacrylate/MMA copolymer due to an increase in crosslink density.

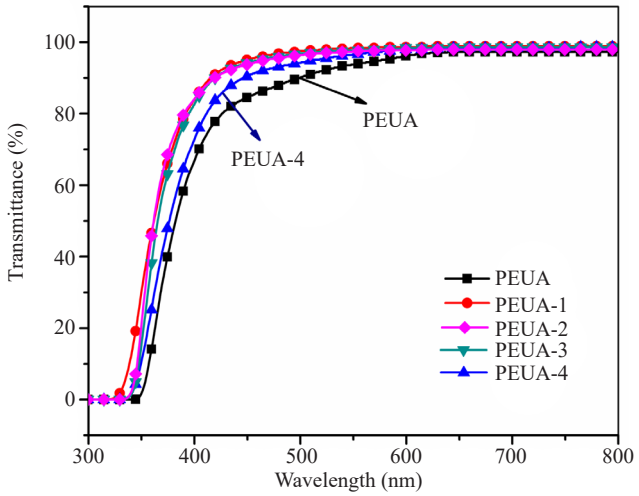

Figure 7. UV-vis spectra of the crosslinked PEUA and its copolymers

Table 5. Transmittance (%) of PEUA and its copolymers at various wavelengths

Sample	Transmittance (%) λ (nm)				
	450	500	550	600	650
PEUA	84.7	90.2	93.6	96.2	97.2
PEUA-1	95.0	97.5	98.4	98.6	98.8
PEUA-2	93.8	96.4	97.5	97.2	98.4
PEUA-3	94.2	96.8	97.2	98.4	98.6
PEUA-4	90.7	94.2	96.6	97.9	98.4

4.7 *Heat deflection temperature*

The short-time thermo mechanical properties of materials can be anlayzed by using HDT analysis. It is the temperature at which a polymer sample deforms under a specified load. The HDT of virgin PEUA and PMMA were found to be 58 °C and 92 °C, respectively. On incorporating MMA into PEUA, the heat deflection temperature of the copolymer was enhanced due to the compatibility of MMA (40 wt%).[35] Table 6 shows a slightly higher experimental value of PEUA-3 in comparison to its theoretical value, while all other PEUA/MMA copolymers had slightly lower values than the theoretical values. This behavior of PEUA-3 we attributed to the higher number of H-bonds which enhanced the stiffness of the system, resulting in lower deflection and higher HDT, as discussed in the FTIR section.

Table 6. Glass transition temperatures (T_g) and heat deflection temperatures of PEUA, PMMA and their copolymers

Composition	Glass transition temperature (T_g) (°C)			Compatibility factor (θ)*		Heat deflection Temperature (°C)	
	By DSC	Calculated by (equation)				Experimental	Calculated**
		Fox	Gordon & Taylor	Fox	Gordon & Taylor		
PMMA	109.4	-	-	-	-	92	-
PEUA	48	-	-	-	-	58	-
PEUA-1	95.1	95.3	97.1	0.0022	0.0212	84	86
PEUA-2	82.3	82.2	84.8	-0.0009	0.0308	78	79
PEUA-3	75.9	70.1	72.5	-0.0773	-0.0440	79	72
PEUA-4	52.1	58.6	60.3	0.1279	0.1592	62	65

* Compatibility factor (θ) was calculated using the equation: T_g(DSC)-T_g(calculated)/T_g(calculated) = -θ/1 + θ

** HDT (°C) calculated by rule of mixtures

4.8 *Differential scanning calorimetry (DSC) analysis of PEUA, PMMA and their copolymer*

The glass transition temperatures (T_g) of all of the copolymers were found to be in between the T_g of PEUA (48 °C) and PMMA (109 °C) (Table 6). The appearance of a single T_g indicated the miscibility of the mers in the copolymer network structure, resulting in a homogeneous, amorphous structure of the copolymer.[36-37] Figure 8 and Table 6 show that with an increase in MMA content the T_g of the PEUA/MMA copolymer increased concerning that of PEUA. PEUA-3 showed a higher experimental value of T_g than the theoretical values, while the PEUA-1 and PEUA-2 had values similar to the theoretical values and PEUA-4 had a lower value. This result indicated the formation of a crosslinked network structure amongst the PEUA molecules that enhanced the stiffness.[38] Table 6 shows a positive deviation in T_g values from the theoretical values PEUA-1 to PEUA-3 copolymer which could be ascribed to specific interactions between the segments of both polymers, whereas the reverse effect was observed in the case of PEUA-4. This might be due to the positive shrinkage of PEUA-3 copolymer as discussed earlier, which resulted in decreasing the free volume and consequently, a higher T_g. The compatibility factor (θ) was calculated based on a theoretical equation as reported by Xiao et al.[39] A decrease in 'θ' implies greater miscibility. PEUA-3 showed a negative 'θ' value which might be due to a greater bonding between PEUA and MMA for its concentration. This could be attributed to the strong network structure in PEUA-3.

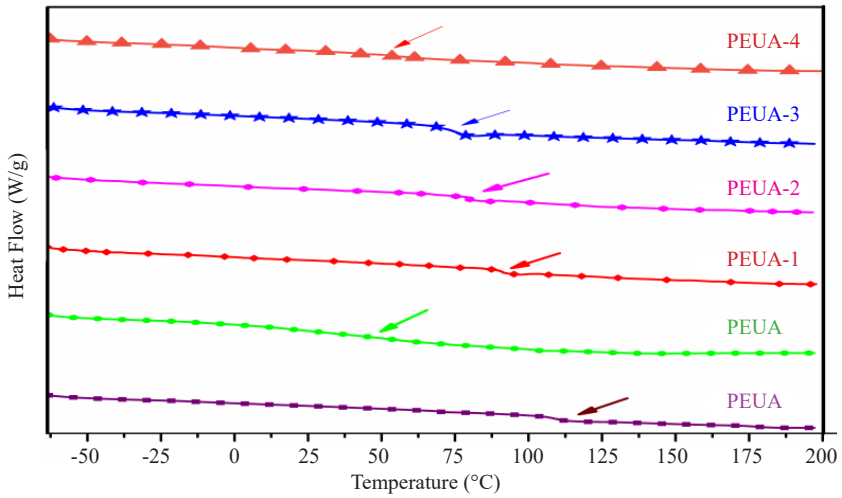

Figure 8. DSC graph of the crosslinked PEUA, PMMA and its copolymers

5. Conclusions

Poly (ester-urethane-acrylate) (PEUA) was prepared by reacting two moles of isophorone diisocyanate (IPDI) with one mole of bis(1,4-butanediol ortho-phthalate) (BPE), followed by end-capping with two moles of 2-hydroxyethyl methacrylate (HEMA) in the presence of dibutyltin dilaurate (DBTDL) catalyst. Thereafter PEUA/MMA copolymers with various compositions were prepared by free radical co-polymerization. FTIR studies confirmed the successful copolymerization and formation of a crosslinked network structure of PEUA/MMA. The 40 wt% MMA containing PEUA copolymer (PEUA-3) showed the lowest volume shrinkage and improved abrasive wear resistance and mechanical, thermal, and optical properties as compared to the other copolymers. Positive polymerization shrinkage of PEUA-1 to PEUA-3 was attributed to the better miscibility between PEUA and MMA, as compared to the negative shrinkage of PEUA-4. The UV-vis spectra showed high transparency of copolymers which thus might be used for optical applications.

Acknowledgment

Financial support given by the Department of Chemicals and Petrochemicals, Ministry of Chemical & Fertilizers, Govt. of India (Letter No. 15012/1/2013-PC-I) is gratefully acknowledged.

Conflict of interest

The authors declare no competing financial interest.

References

[1] Maurya, S. D.; Kurmvanshi, S. K.; Mohanty, S.; Nayak, S. K. *Polymer-Plastics Tech. and Eng.* **2018,** *57*, 625-656.
[2] Bahadur, A.; Shoaib, M.; Saeed, A.; Iqbal, S. *e-Polymers* **2016,** *16*, 463-474.
[3] Gao, L.; Zhou, L.; Fang, S.; Wu, C.; Guo, L.; Sun, G.; Ma, S. *J. of Polymer Research* **2011,** *18*, 833-841.
[4] Das, S.; Pandey, P.; Mohanty, S.; Nayak, S. K. *Polymer-Plastics Tech. and Eng*. **2017,** *56*, 1556-1585.
[5] Fang, S.; Gao, L.; Zhou, L.; Zheng, Z.; Guo, B.; Zhang, C. *J of Applied Poly. Scie*. **2009,** *111*, 724-729.
[6] Digar, M. L.; Hung, S. L.; Wen, T. C.; Gopalan, A. *Polymer* **2002,** *43*, 1615-1622.
[7] Ji, F. L.; Hu, J. L.; Yu, W. M. W.; Chiu, S. S. Y. *J. of Macr. Scie., Part B* **2011,** *50*, 2290-2306.
[8] Nachman, M.; Kwiatkowski, K. *Wear* **2013,** *306*, 113-118.
[9] Oh, Y. S.; Kim, S. R.; Lee, S.; Lee, J. O.; Kim, B. K. *J. of Macr. Scie., Part B* **1995,** *34*, 199-214.
[10] Maurya, S. D.; Kurmvanshi, S. K.; Mohanty, S.; Nayak, S. K. *Macromolecular Research* **2017,** *25*, 871-881.
[11] Lin, S. P.; Shen, J. H.; Han, J. L.; Lee, Y. J.; Liao, K. H.; Yeh, J. T.; Hsieh, K. H. *Comp. Scie. and Tech*. **2008,** *68*, 709-717.
[12] Schaeffer, W. R. *Radtech-North America* **2002,** 1-8. https://citeseerx.ist.psu.edu/document?repid=rep1&type=pdf&doi=ab17bb60e8e111663bacda1299767831aecf9eb9.
[13] Harikrishna, R.; Bhosle, S. M.; Ponrathnam, S.; Rajan, C. R. *J. of Mat. Sci*. **2011,** *46*, 2221-2228.
[14] Kulawska, M.; Moroz, H.; Kasprzyk, A. *Reaction Kinetics, Mech. and Cat.* **2011,** *104*, 9-15.
[15] Maurya, S. D.; Purushothaman, M.; Krishnan, P. S. G.; Nayak, S. K. *J. of Thermoplastic Comp. Mat.* **2014,** *27*, 1711-1727.
[16] Xu, H.; Zheng, X.; Huang, Y.; Wang, H.; Du, Q. *Langmuir* **2016,** *32*, 38-45.
[17] Jian, Y.; He, Y.; Jiang, T.; Li, C.; Yang, W.; Nie, J. *J. of Coat. Tech. and Res*. **2013,** *10*, 231-237.
[18] Maurya, S. D.; Kurmvanshi, S. K.; Mohanty, S.; Nayak, S. K. *J. of Macr. Sci., Part A* **2018,** *55*, 1-10.
[19] Brostow, W.; Chiu, R.; Kalogeras, I. M.; Vassilikou-Dova, A. *Materials Letters* **2008,** *62*, 3152-3155.
[20] Fox, T. G. *Bull. Am. Phs. Soc*. **1952,** *1*, 123.
[21] Gordon, M.; Taylor, J. S. *J. of App. Chem.* **1952,** *2*, 493-500.
[22] Pavia, D. L.; Lampman, G. M.; Kriz, G. S.; Vyvyan, J. A. *Introduction to Spectroscopy, Cengage Learning*, 4th Edn., Cengage Learning; Library of Congress Control, 2008; pp 745.

[23] Huang, J.; Zhang, L. *Polymer* **2002,** *43*, 2287-2294.
[24] Gilbert, J. L.; Hasenwinkel, J. M.; Wixson, R. L.; Lautenschlager, E. P. *J. of Biomedical Mat. Res*. **2000,** *52*, 210-218.
[25] Jian, Y.; He, Y.; Zhao, L.; Kowalczyk, A.; Yang, W.; Nie, J. *Adv. in Poly. Tech.* **2013,** *32*, 1-9.
[26] Wen, M.; Scriven, L. E.; McCormick, A. V. *Macromolecules* **2002,** *35*, 112-120.
[27] Chen, S.; Wang, Q.; Wang, T. *Tribology Letters* **2011,** *43*, 319-327.
[28] Li, B.; Li, M.; Fan, C.; Ren, M.; Wu, P.; Luo, L.; Liu, X. *Comp. Sci. and Tech.* **2015,** *106*, 68-75.
[29] Mishra, V.; Mohanty, I.; Patel, M. R.; Patel, K. I. *I. J. of Poly. Any. and Char.* **2015,** *20*, 504-513.
[30] Sultan, M.; Bhatti, H. N.; Zuber, M.; Barikani, M. *Korean J. of Chem. Eng*. **2013,** *30*, 488-493.
[31] Vasoya, P. J.; Parsania, P. H. *Polymer-Plastics Tech. and Eng*. **2008,** *47*, 635-642.
[32] Sakurai, T.; Sugawara, I.; Niwa, M.; Tanaka, H. *Desi. Mono. and Poly*. **2013,** *16*, 358-365.
[33] Tyagi, A. K.; Choudhary, V.; Varma, I. K. *Euro. Poly. J.* **1994,** *30*, 919-924.
[34] Ballestero, R.; Sundaram, B. M.; Tippur, H. V.; Auad, M. L. *eXPRESS Polymer Letters* **2016,** *10*, 204-215.
[35] Faris, T. V.; Gordon, G. T.; Chan, D. T. *U.S. Patent* **2003,** 6653405B2.
[36] Chen, R.; Zhang, C.; Kessler, M. R. *RSC Advances* **2014,** *4*, 35476-35483.
[37] Ali, K. I.; Sasaki, T. *Rad. Phy. and Che*. **1994,** *43*, 371-375.
[38] Zhang, J. L.; Wu, D. M.; Yang, D. Y.; Qiu, F. X. *J. of Poly. and Envi*. **2010,** *18*, 128-134.
[39] Xiao, H. X.; Frisch, K. C.; Frisch, H. L. *J. of Poly. Sci.: Poly. Che*. **1983,** *21*, 2547-2557.